Theoretical Study of the Relativistic Effects on the Bonds between $HfCl_3$ and H and between $ThCl_3$ and H

Egbert M. Wezenbeek,[†] Evert Jan Baerends,*[,†] and Tom Ziegler*[,‡]

Department of Theoretical Chemistry, Vrije Universiteit, 1081 HV Amsterdam, The Netherlands, and Department of Chemistry, University of Calgary, Calgary, Alberta, Canada

Received March 30, 1994[⊗]

The relativistic effects on the bonds between H and MCl_3 (M = Hf, Th) in Cl_3M-H were investigated by comparing results from nonrelativistic (NR) and quasirelativistic (QR) calculations on the title systems. The calculations were carried out in order to better understand the differences between ligand−metal σ-bonds involving early transition metals and metal−ligand σ-bonds involving f-block elements. The bonding between the transition metal fragment $HfCl_3$ and H is qualitatively the same in the nonrelativistic and quasirelativistic pictures: 5d contributes in both cases more to the bond than 6s. Nonrelativistically, 6s is more stable than 5d by −0.61 eV. Still, 5d has a larger contribution to the bond since it has a numerically larger interaction matrix element with H 1s. The 6s−5d gap is increased by relativity to 2.73 eV. Nevertheless, 5d is still the dominant component in the QR bonding picture, although the 6s contribution has increased slightly. In the heavier actinide system $ThCl_3H$ there are large differences between the NR and QR bonding pictures. Nonrelativistically 5f and 6d are the dominant metal components in the bonding to H whereas 6d is the principal metal component in the quasirelativistic case. The 7s orbital hardly contributes to the bond with H in either of the calculations. In the NR case the 5f orbital participates in the bonding since it is 5.27 eV below 6d and 6.29 eV below 7s. However, 6d has as strong a contributing role, although it is of higher energy, since it has a numerically large interaction matrix element with H 1s. Relativistic effects destabilize 5f by 6.46 eV. Now 7s is 1.04 eV below 5f and 1.32 eV below 5d. The destabilization of 5f removes it from the bond to hydrogen and makes 6d the only strongly participating metal orbital. It is concluded that relativity is important for even a qualitatively correct description of σ-bonds involving actinides. Also the Hf−H and Th−H bonds become quite similar after relativity has been included in the description of the latter.

Introduction

In the last decade calculations including relativistic effects on molecules have become almost routine.[1−7] Out of the large number of schemes available, we mention methods based on first-order perturbation theory (FOPT),[2] the quasirelativistic (QR) approach,[3,4] the basis set expansion method to solve the Dirac Hamiltonian,[6a−c] relativistic effective core-potential schemes,[6d−e] as well as all electron variational two-component methods based on the Douglas−Kroll[7a−c] and other regularized Hamiltonians.[7d−f]

The simplest of the relativistic schemes is likely the FOPT approach. This method neglects energy contributions from relativistic changes in the electronic density as well as other terms of second and higher order in α^2, where α is the fine structure constant. It has been shown that FOPT is adequate in calculations on dissociation energies for bonds involving elements up to Au and Hg ($Z = 80$)[3,5] in spite of the approximations involved. However, FOPT fails in calculations of dissociation energies for bonds involving elements heavier than mercury such as the actinides.[5] For these elements relativistic corrections significantly change the relative energies of the 7s, 6d, and 5f AO's,[4,5] and thus the bonding picture. A next step up from the FOPT approach is the QR scheme,[4,5] in which changes in the density induced by the first-order relativistic Hamiltonian are taken into account in the bond energy calculations to all orders in α^2, whereas relativistic operators to second and higer orders are neglected. We have shown in a previous study[5] that the QR method is able to provide accurate estimates of bond energies involving elements as heavy as the actinides. However, this numerical study[5] did not provide an examination of how relativity modifies the electronic structure and strength of bonds involving 5f elements. It is the aim of the present investigation to provide such an analysis.

One of the more important fragments in the emerging field of organoactinide chemistry[8a] is AcL_3 with L represented by halides or cyclopentadienyl (Cp) rings. This fragment is bound

[†] Vrije Universiteit.

[‡] University of Calgary.

[⊗] Abstract published in *Advance ACS Abstracts,* November 15, 1994.

(1) (a) Baerends, E. J.; Ellis, D. E.; Ros, P., *Chem. Phys.* **1973**, *2*, 42. (b) Baerends, E. J.; Ros, P. *Chem. Phys.* **1973**, *2*, 51. (c) Baerends, E. J.; Ros, P. *Int. J. Quantum Chem.* **1978**, *S12*, 169.

(2) (a) Snijders, J. G.; Baerends, E. J. *Mol. Phys.* **1978**, *36*, 1789. (b) Snijders, J. G.; Baerends, E. J.; Ros, P. *Mol. Phys.* **1979**, *38*, 1909.

(3) Ziegler, T.; Snijders, J. G.; Baerends, E. J. *Chem. Phys.* **1981**, *74*, 1271.

(4) Boerrigter, P. M. Ph.D. Thesis, Vrije Universiteit, Amsterdam, 1987.

(5) Ziegler, T.; Baerends, E. J.;Snijders, J. G.; Ravenek, W. *J. Phys. Chem.* **1989**, *93*, 3050.

(6) (a) Ishikawa,Y.; Binning, R. C.; Sando, K. M. *Chem. Phys. Lett.* **1983**, *101*, 111. (b) Aerts, P. J. C.; Nieuwpoort, W. C. *Chem. Phys. Lett.* **1985**, *113*, 165. (c) Grant, I. P. *J. Phys. B: At. Mol. Phys.* **1986**, *19*, 3187. (d) Christiansen, P. A.; Ermler, W. C.; Pitzer, K. *Annu. Rev. Phys. Chem.* **1985**, *38*, 407. (e) Hafner, P.; Schwarz, W. H. E. *J. Phys. B: At. Mol. Phys.* **1978**, *11*, 217.

(7) (a) Hess, B. A. *Phys. Rev.* **1986**, *A33*, 3742. (b) Douglas, M.; Kroll, N. M. *Ann. Phys.* **1974**, *82*, 89. (c) Knappe, P.; Rösch, N. J. *Chem. Phys.* **1990**, *92*, 1153. (d) Chang, Ch.; Pelissier, M.; Durand, Ph. *Phys. Scr.* **1986**, *34*, 394. (e) Heully, J. L.; Lindgren, I.; Lindroth, E.; Lundqvist, S; Martensson-Pendrill, A. M. *J. Phys.* **1986**, *B19*, 2799. (f) van Lenthe, E.; Baerends, E. J.; Snijders, J. G. *J. Chem.Phys.* **1993**, *99*, 4597.

(8) (a) Gulino, A.; Ciliberto, E.; Bella, S. D.; Fragalo, I.; Seyam, A. M.; Marks, T. *Organometallics* **1992**, *11*, 3248 and references therein. (b) Strittmatter, R. J.; Bursten, B. E. *J. Am. Chem. Soc.* **1991**, *113*, 552. (c) Bursten, B. E.; Rhodes, L. F.; Strittmatter, R. J. *J. Am. Chem. Soc.* **1989**, *111*, 2758. (d) van Wezenbeek, E. M. Thesis Free University, Amsterdam, 1992.

0020-1669/95/1334-0238$09.00/0

Table 1. Irreducible Representations of Orbitals in Symmetry C_{3v}

representation	Cl_3 combination	metal orbitals
A_1	3s, $3p_\sigma$, and $3p_\pi$	s, p_z (p_σ); d_{z^2} (d_σ) f_{z^3} (f_σ), $f_{x(x^2-3y^2)}$ (f_ϕ)
A_2	$3p_\pi$	$f_{y(3x^2-y^2)}$ (f_ϕ)
E	3s, $3p_\sigma$, and $3p_\pi$ (twice)	p_x, p_y (p_π) d_{xz}, d_{yz} (d_π); $d_{x^2-y^2}$, d_{xy} (d_δ) f_{xyz}, f_z (f_δ)

by a single bond to a variety of one-electron ligands, X, as L_3-Ac−X. We shall study Cl_3Th−H as a representative for this class of important compounds. The emphasis will be on the Th−H bond and the way in which it is modified by relativity. We shall further make comparisons to the corresponding σ-bond in the isoeletronic Cl_3Hf−H system where the metal center is represented by an early 5d transition metal rather than a 5f element. The important status of the AcL_3 fragment has already prompted a number of studies on its electronic structure.[8] Most recently Strittmatter and Bursten[8b] have studied the bonding in Cp_3Ac for a series of actinides using a relativistic Xα−SW method. The same method was also used to study the bonding in Cp_3U−L with L = H, NO and CO.[8c] However, this scheme is not able to provide estimates of bond energies. Also, the Xα−SW method is not amenable to the type of population analysis one can perform with methods based on basis sets. Fragala, Marks,[8a] and co-workers have studied the photoelectron spectra of Cp_3U−X molecules supplemented with DV−Xα calculations. This study has the strongest bearings on the present investigation. However, the Xα calculations were carried out without relativistic corrections.

Computational Details

The molecules considered all have C_{3v} symmetry, for which the irreducible representations of the atomic orbitals are given in Table 1. We are only interested in the A_1 symmetry, where the interaction with H takes place. The Cl 3s and 3p orbitals lead to A_1, A_2, and E combinations. In A_1 symmetry we have the 3s, $3p_\sigma$, and $3p_\pi$ bonding combinations. Only the 3p combinations are involved in the bond with the metal; the 3s lies too deep in energy. Note that in A_1 symmetry we have the metal orbitals s, p_σ, d_σ, f_σ, and one f_ϕ ($f_{x(x^2-3y^2)}$) component. The structures of $HfCl_3H$[9] and $ThCl_3H$ were fully optimized. The estimated QR bond distances are R(Hf−Cl) = 2.35 Å, R(Hf−H) = 1.80 Å, R(Th−Cl) = 2.58 Å, and R(Th−H) = 2.09 Å.

The calculations reported in this work have been carried out with the Amsterdam DFT program system[1] ADF, which incorporates relativistic extensions first developed by Snijders et al.[2] The LDA exchange potential was used[10] together with the Vosko−Wilk−Nusair[11] parametrization for correlation, omitting the correlation between electrons of equal spin, as suggested by Stoll.[12] For the bonding between the open-shell fragments MCl_3 and H we used the extended transition state method[13a] (ETS), which was recently extended to open-shell systems.[13b]

The ETS scheme divides the bond energy into two parts as

$$D(\mathrm{M-X}) = \Delta E^0 + \Delta E_{\mathrm{oi}} \qquad (1)$$

The first part, ΔE^0, represents the total steric interaction between H and the MCl_3 fragment. It can be decomposed further according to

$$\Delta E^0 = \Delta E_{\mathrm{el.stat}} + \Delta E_{\mathrm{Pauli}} \qquad (2)$$

where $\Delta E_{\mathrm{el.stat}}$ is the electrostatic interaction between H and MCl_3 whereas $\Delta E_{\mathrm{Pauli}}$ represents the repulsive interaction between the occupied 1s orbital on hydrogen (of, e.g., β-spin) and occupied orbitals on MCl_3 with the same (β-)spin polarization. The Pauli repulsion is in general the result of (destabilizing) interactions between occupied orbitals of the same spin.[14]

The second term in eq 1, ΔE_{oi}, represents the stabilizing interaction between occupied and virtual fragment orbitals. For closed-shell fragments, this term takes into account charge transfer and polarization energies,[13c] but for open-shell fragments also the effect of the pair bond formation is included. The pair bond formation involves in the present case the two singly occupied orbitals FO_{MCl_3} and H 1s. If the basis functions are symmetry (Γ) adapted, the orbital interaction can be decomposed according to[13a,d]

$$\Delta E_{\mathrm{oi}} = \sum_{\Gamma} \Delta E_{\mathrm{oi}}^{\Gamma} \qquad (3)$$

Relativity was taken into account using the quasirelativistic method[5] in which the relativistic mass velocity (h_{MV}) and Darwin (h_{D}) corrections are added to the nonrelativistic one-electron equations. In the QR method changes in the valence density induced by $h_{\mathrm{MV}} + h_{\mathrm{D}}$ are taken into account in the bond energy calculations to all orders in α^2, whereas relativistic operators to second and higer orders are neglected.

The metal centers were represented by a triple-ζ STO basis[15] set for 5s,5p,5f,6s,6p on Hf and 5f,6s,6p,6d,7s,7p on Th. Levels of lower energy were treated by the frozen-core approximation. A double-ζ STO basis[15] was adopted for Cl and H augmented by a single 3d (Cl) or 2p (H) STO. The Cl $1s^2 2s^2 2p^6$ configuration was treated as core. A set

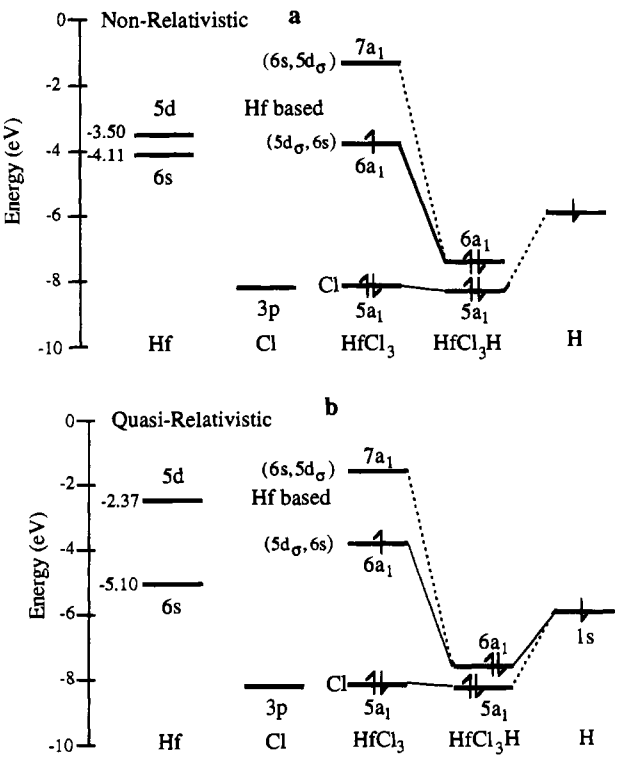

Figure 1. Level schemes for the Hf compounds: (a) nonrelativistic; (b) quasirelativistic.

(9) Ziegler, T.; Tschinke, V.; Versluis, L.; Baerends, E. J.; Ravenek, W. *Polyhedron* **1988**, *7*, 1625.
(10) (a) Parr, R. G.; Yang, W. *Density-Functional Theory of Atoms and Molecules*; Oxford University Press: New York, 1989. (b) Ziegler, T. *Chem. Rev.* **1991**, *91*, 651.
(11) Vosko, S. H.; Wilk, L.; Nusair, M. *Can. J. Phys.* **1980**, *58*, 1200.
(12) Stoll, H.; Golka, E.; Preus, H. *Theor. Chim. Acta* **1980**, *29*, 29.
(13) (a) Ziegler, T.; Rauk, A. *Theor. Chim. Acta* **1977**, *46*, 1. (b) Bickelhaupt, F. M.; Nibbering, N. M. M.; van Wezenbeek, E. M.; Baerends, E. J. *J. Phys. Chem.* **1992**, *96*, 4864. (c) Kitaura, K.; Morokuma, K *Int. J. Quantum. Chem.* **1976**, *10*, 325. (d) Ziegler, T. *NATO ASI* **1992**, *C378*, 367.
(14) Albright, T. A.; Burdett, J. K.; Whangbo, M. H. Orbital Interactions in Chemistry; Wiley: New York, 1985.
(15) (a) Snijders, G. J.; Baerends, E. J.; Vernooijs, P. *At. Nucl. Data Tables* **1982**, *26*, 483. (b) Vernooijs, P.; Snijders, G. J.; Baerends, E. J. Slater Type Basis Functions for the whole Periodic System. Internal Report, Free University of Amsterdam, The Netherlands, **1984**.

Table 2. Population Analysis for Some A_1 Orbitals of $HfCl_3$

NR	Orbital	Orbital character	Energy (eV)	%Hf-contribution			%Cl-contribution	
				6s	$6p_\sigma$	$5d_\sigma$	p_σ	p_π
	$7a_1^f$ 0.0	$(s\text{–}Clp_\sigma)\text{–}(d_\sigma\text{–}Clp_\pi)$	−1.39	44	25	21	5	5
	$6a_1^f$ 1.0	$(d_\sigma\text{–}Clp_\pi)+(s\text{–}Clp_\sigma)$	−3.77	26	6	64	1	3
	$5a_1^f$	Cl (-d_σ bond)	−8.13		2	5	4	89
	$4a_1^f$	Cl (- s,d_σ bond)	−9.14	7		5	84	2
Gross Populations				0.42	0.10	0.84	1.87	1.86

QR	Orbital	Orbital character	Energy (eV)	%Hf-contribution			%Cl-contribution	
				6s	$6p_\sigma$	$5d_\sigma$	p_σ	p_π
	$7a_1^f$ 0.0	$(s\text{–}Clp_\sigma)\text{–}(d_\sigma\text{–}Clp_\pi)$	−1.53	32	19	35	8	7
	$6a_1^f$ 1.0	$(d_\sigma\text{–}Clp_\pi)+(s\text{–}Clp_\sigma)$	−3.95	39	7	51	1	3
	$5a_1^f$	Cl (-d_σ bond)	−8.19		3	5	1	91
	$4a_1^f$	Cl (- s,d_σ bond)	−9.73	14		3	80	1
Gross Populations				0.73	0.13	0.67	1.64	1.84

of auxiliary s, p, d, f, and g STO functions,[16] centered on all nuclei, was used to fit the molecular density and represent Coulomb and exchange potentials accurately in each SCF cycle.

Results and Discussion

(a) Influence of Relativity on the Atomic Orbitals of Hf and Th. The NR and QR atomic energy levels of Hf and Th are given in Figures 1 and 2. The familiar atomic relativistic effects are found: stabilization of $(n + 1)$s orbitals and destabilization of nd and $(n - 1)$f orbitals.[17,18] The assumed valence orbital occupation in both cases is $(n + 1)s^2nd^2$. Also the energy levels of MCl_3 and MCl_3H are indicated in these figures.

Electrons in the valence $(n + 1)$s orbitals can penetrate to the nucleus and thus obtain high instantaneous velocities which will result in substantial kinetic energies. However, relativity will reduce the kinetic energy to some extent through the mass velocity term h_{MV} as a result of the well-known relativistic mass increase.[3,17,18] The end result is a relativistic stabilization and contraction of the $(n + 1)$s orbital. Thus, for $(n + 1)$s relativity is seen to have a direct influence on the energy and radial extent of the orbital. Electrons in the valence nd and $(n - 1)$f orbitals do not penetrate to the nucleus where they can acquire high instantaneous velocities. These orbitals are as a consequence not subject to the same direct relativistic effects as $(n + 1)$s. However, the contraction of the core orbitals due to the relativistic reduction in kinetic energy of the core electrons will reduce the effective nuclear charge experienced by nd and $(n - 1)$f, with the result that these valence orbitals are destabilized and expanded.[17,18] The destabilization of nd and $(n - 1)$f is referred to as the indirect relativistic effect.

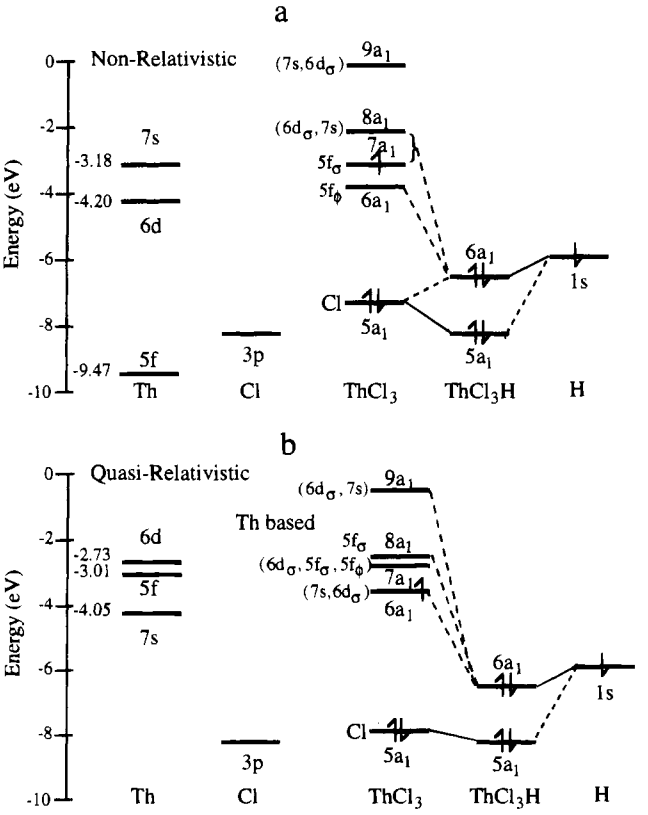

Figure 2. Level schemes for the Th compounds: (a) nonrelativistic; (b) quasirelativistic.

For Hf, the valence level ordering is 6s below 5d, with an energy difference of 0.61 eV in the NR case, but in the QR

(16) Krijn, M. P. C. M.; Baerends, E. J. Fit Functions in the HFS Method. Internal Report (in Dutch), Free University of Amsterdam, The Netherlands, 1984.
(17) Pyykkö, P. *Chem. Rev.* **1988**, *88*, 563.
(18) Schwarz,W. H. E.; van Wezenbeek, E. M.; Baerends, E. J.; Snijders, J. G. *J. Phys.* **1989**, *B22*, 1515.

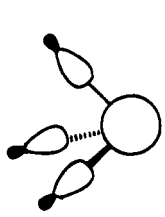

$\langle (n+1)S \mid Cl_\sigma \rangle$:

	NR	QR
Hf	0.37	0.42
Th	0.24	0.32

1a

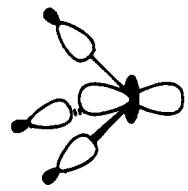

$\langle d_\sigma \mid Cl_\sigma \rangle$:

	NR	QR
Hf	-0.10	-0.12
Th	-0.10	-0.11

1b

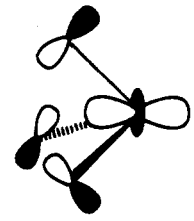

$\langle d_\sigma \mid Cl_\pi \rangle$:

	NR	QR
Hf	0.18	0.21
Th	0.19	0.22

1c

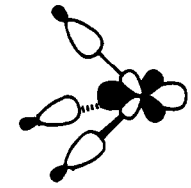

$\langle f_\sigma \mid Cl_\sigma \rangle$:

	NR	QR
Th	0.04	0.05

1d

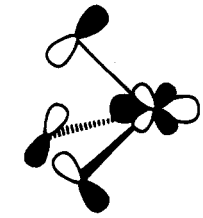

$\langle f_\sigma \mid Cl_\pi \rangle$:

	NR	QR
Th	0.02	0.03

1e

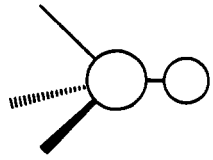

$\langle (n+1)S \mid 1s_H \rangle$:

	NR	QR
Hf	0.48	0.48
Th	0.40	0.42

1f

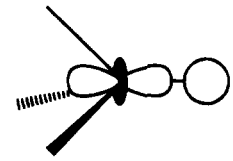

$\langle d_\sigma \mid 1s_H \rangle$:

	NR	QR
Hf	0.31	0.34
Th	0.35	0.38

1g

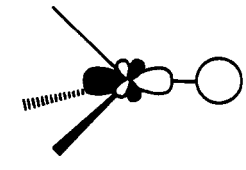

$\langle f_\sigma \mid 1s_H \rangle$:

	NR	QR
Th	0.07	0.10

1h

calculation the energy difference has increased to 2.73 eV, as a result of the stabilization of 0.99 eV for Hf 6s and the destabilization of 1.13 eV for Hf 5d, Figure 1.

For the heavier Th the situation is completely different. The order is 5f < 6d < 7s in the NR case, while in the QR scheme it is 7s < 5f < 6d. The main reason for this change is the large indirect destabilization of 6.46 eV for Th 5f, while Th 6d also has a considerable destabilization of 1.47 eV. With the 0.87 eV stabilization of Th 7s, the order of 7s and 6d is reversed, and 5f ends up between 7s and 6d, Figure 2.

(b) Metal−Ligand Overlaps in $HfCl_3$ and $ThCl_3$. For a proper understanding of the interaction between MCl_3 and H in MCl_3H, we first discuss the MCl_3 fragments. As both the MCl_3 and MCl_3H compounds have C_{3v} symmetry, we distinguish the orbitals of the MCl_3 fragments by a superscript f (for fragment). Furthermore, since the interaction with H takes place in A_1 symmetry, only the 6s and $5d_\sigma$ orbitals on Hf and the 7s, $6d_\sigma$, and $5f_{\sigma,\phi}$ orbitals in Th are involved, Table 1. Overlaps between normalized Cl_3 combinations and H 1s with atomic orbitals of Hf and Th are given in **1a−h**. The phases of the metal orbitals were chosen such that the $(n + 1)$s orbital was positive, and for the nd and $(n - 1)$f orbitals the lobes pointing toward H were positive. The Clp_σ combination has the positive lobes directed toward the metal. We note in addition that the d_σ−Clp_σ overlaps, **1b**, are negative, and much smaller than the d_σ−Clp_π counterparts, **1c**. This is a consequence of the nodal character of the nd_σ orbital. The Clp_σ orbital overlaps, **1b**, mainly with the central lobe of d_σ, but this is partly cancelled by overlap with the outside lobe. As expected, the overlaps of the $(n + 1)$s orbitals with the Clp_π combinations are zero.

The effects of relativity on the overlaps, **1a−h**, are rather small. The relativistic expansion of the nd and $(n - 1)$f orbitals leads to growths in the overlaps with Clp_σ, **1b** and **1d**, and Clp_π, **1c** and **1e**, as well as H 1s, **1g** and **1h**. At the same time, the relativistic contraction of the $(n + 1)$s orbital is seen to enhance the overlap with p_σ, **1a**, and H 1s, **1f**. Thus, overlaps increase whether the atomic metal orbitals are contracted or expanded by relativity. In the case of nd and $(n - 1)$f, both orbitals are rather contracted and an expansion will bring their radial maximum closer to the M−Cl bond midpoint and the hydrogen center. The $(n + 1)$s orbital is on the other hand diffuse with a maximum beyond the M−Cl bond midpoints and the M−H bond distance. It is thus not surprising that a contraction will lead to larger overlaps in **1a** and **1f.**

(c) The Singly Occupied Frontier Orbital in $HfCl_3$ and $ThCl_3$. The electronic structure in ML_3 systems of early transition metals and f-block elements has been discussed previously.[8b] The lower lying levels in ML_3 are all ligand based and represented by nonbonding or slightly bonding orbitals with small contributions from the metal center. At higher energy are the metal-based antibonding combinations, Figures 1 and 2. We shall here concentrate on the nature of the singly occupied metal-based frontier orbital denoted $6a_1$ in Figures 1 and 2. Tables 2 and 3 provide an analysis of the composition for $6a_1$ and other A_1 orbitals of $HfCl_3$ and $ThCl_3$.

The nonrelativistic (NR) $6a_1$ orbital of $HfCl_3$, **2a**, is mainly (64%) $5d_\sigma$ in nature with some (26%) 6s character and antibonding contributions from Cl_σ (1%) and Cl_π (3%). Rela-

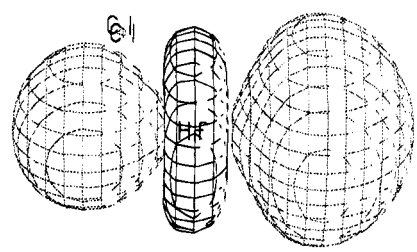

2a

tivity primarily modifies the $6a_1$ orbital, **2b**, by increasing the

Table 3. Population Analysis for Some A_1 Orbitals of $ThCl_3$

NR	Orbital	Orbital character	Energy (eV)	%Th-contribution				%Cl-contribution	
				7s	$6d_\sigma$	$5f_\sigma$	$5f_\phi$	p_σ	p_π
	$9a_1^f$	$(s–Clp_\sigma)–(d_\sigma–Clp_\pi)$	–0.22	44	28	2	4	3	2
	$8a_1^f$0.0	$(d_\sigma–Clp_\pi)+(s–Clp_\sigma)$	–2.10	38	57				3
	$7a_1^f$1.0	f_σ -Cl b.	–3.13	3	1	92		1	1
	$6a_1^f$0.0	f_ϕ	–3.69	4	2	2	88	3	
	$5a_1^f$	Cl	–7.27	1	1	2		61	22
	$4a_1^f$	Cl -(d_σ, f_ϕ bond)	–7.92	1	6		5	23	71
Gross Populations				0.09	0.16	0.99	0.15	1.74	1.89

QR	Orbital	Orbital character	Energy (eV)	% Th-contribution				% Cl-contribution	
				7s	$6d_\sigma$	$5f_\sigma$	$5f_\phi$	p_σ	p_π
	$9a_1^f$	$(d_\sigma–Clp_\pi)-(s–Clp_\sigma)$	–0.47	28	22	6	16	6	2
	$8a_1^f$	5f	–2.56		1	66	32		1
	$7a_1^f$0.0	$(d_\sigma–Clp_\pi)-(s–Clp_\sigma)$	–2.82	1	40	23	34		3
	$6a_1^f$1.0	$(s–Clp_\sigma)+(d_\sigma–Clp_\pi)$	–3.48	60	24	3	12		2
	$5a_1^f$	Cl ($-d_\sigma$ bond)	–7.82	1	4	1		6	88
	$4a_1^f$	Cl -(s, d_σ) bond)	–8.81	7	4	1	3	78	4
Gross Populations				0.79	0.41	0.07	0.20	1.69	1.87

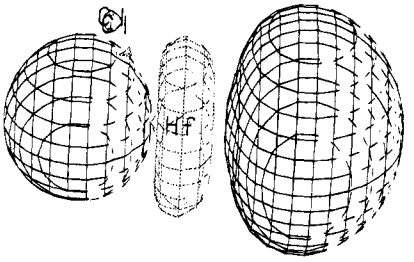

2b

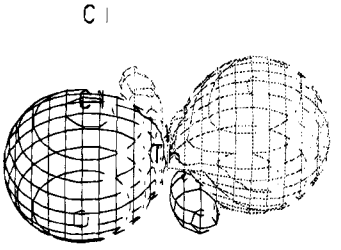

3a

6s contribution (39%) and reducing the d_σ component (51%) as the 6s orbital is stabilized compared to 5d, Figure 1. The increase in the 6s participation can be related to the relativistic stabilization of that orbital, Figure 1.

In the NR calculation on $ThCl_3$, $6a_1$ is a $5f_\phi$ orbital (88%) whereas $7a_1$ is made up of $5f_\sigma$ (92%), **3a**; see Table 2. Thus, the NR frontier orbitals in $ThCl_3$ are f-based whereas the corresponding orbitals in $HfCl_3$ are dominated by 5d and 6s. The dominance of 5f in the frontier orbitals of NR $ThCl_3$ is related to the low nonrelativistic energy of the 5f level. The introduction of relativity stabilizes 7s relative to 6d and (in particular) 5f as discussed before, Figure 2. Now $6a_1$ is mostly 7s (60%), **3b**, whereas the largest metal contribution to $7a_1$ comes from the 5f orbitals (40%), Table 2. Thus, changes in the ordering of the atomic metal orbitals induced by relativity are directly reflected in the way in which relativity modifies the composition of the frontier orbitals in $ThCl_3$. We shall in

Table 4. Population Analysis of Highest Occupied A_1 Orbitals of $HfCl_3H$

NR	Orbital	Orbital char.	Energy (eV)	%Hf-contr.			%$HfCl_3$-contr.				%H-contr.
				6s	6p	5d	$4a_1^f$	$5a_1^f$	$6a_1^f$	$7a_1^f$	
	$6a_1$	5d,6s-H b.	−7.37	5	4	22		6	37	2	59
	$5a_1$	$5a_1^f$-H b.	−8.48	1	2	10		94	6		4
	$4a_1$	$4a_1^f$	−9.39	6		4	98				1
Gross Populations				0.22	0.12	0.73					1.27

QR	Orbital	Orbital char.	Energy (eV)	%Hf-contr.			%$HfCl_3$-contr.				%H-contr.
				6s	6p	5d	$4a_1^f$	$5a_1^f$	$6a_1^f$	$7a_1^f$	
	$6a_1$	5d,6s-H b.	−7.56	6	6	20		7	38	1	53
	$5a_1$	$5a_1^f$-H b.	−8.45	1	2	11		93	1		4
	$4a_1$	$4a_1^f$	−9.94	16		1	97				2
Gross Populations				0.50	0.16	0.65					1.22

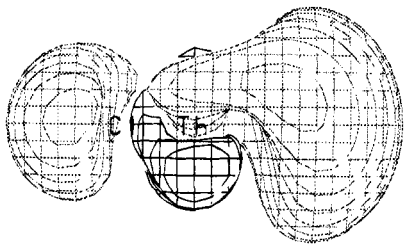

3b

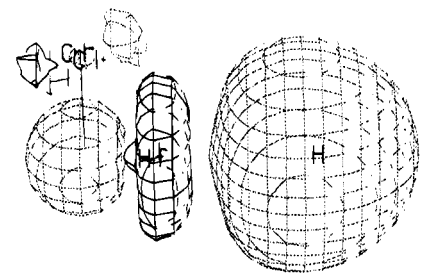

4a

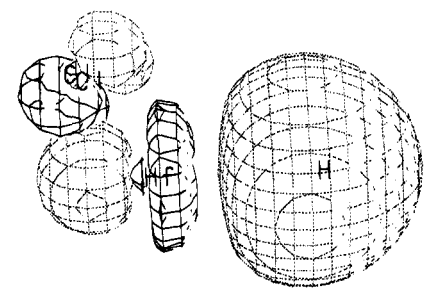

4b

the next section explore how the same changes in the ordering of the atomic metal levels influence the M−H bond in Cl_3M−H with M = Hf and Th.

(d) The Cl_3Hf−H Bond. Level diagrams for $HfCl_3H$ are outllined in Figure 1 on the basis of the orbital interactions between $HfCl_3$ and H. A Mulliken population analysis of the resulting orbitals along with their bonding characteristics is given in Table 4. Note that the bond between $HfCl_3$ and H mainly is a pair bond between the $HfCl_3$ $6a_1^f$ fragment orbital and H 1s. The pair bond is essentially represented by the bonding $6a_1$ HOMO, **4a** (NR) and **4b** (QR). The lower lying $4a_1$ and $5a_1$ levels are represented by nearly pure $HfCl_3$ fragment orbitals, Table 4.

For NR $HfCl_3H$ the gross metal Mulliken populations are 0.73 for 5d and 0.22 for 6s. A comparison with the corresponding populations in $HfCl_3$, Table 2, indicates a loss of 0.11e from 5d and 0.20e from 6s on formation of the Hf−H bond. Thus, relatively more charge is transferred from 6s to H 1s than from 5d. The greater reduction in 6s character can be explained by the fact that 5d has a larger interaction matrix element with 1s than the 6s orbital in absolute terms, although the 6s overlap with H 1s, **1f**, is larger than the overlap between 5d and H 1s, **1g**. A more detailed discussion of this point can be found in ref 8d.

In the QR gross Mulliken population for $HfCl_3H$ 0.50e is associated with 6s and 0.65e with 5d. Thus, the relativistic stabilization of 6s has increased the 6s contribution as expected compared to the NR $HfCl_3H$ complex. However, the calculated difference between the QR gross populations of $HfCl_3$ and

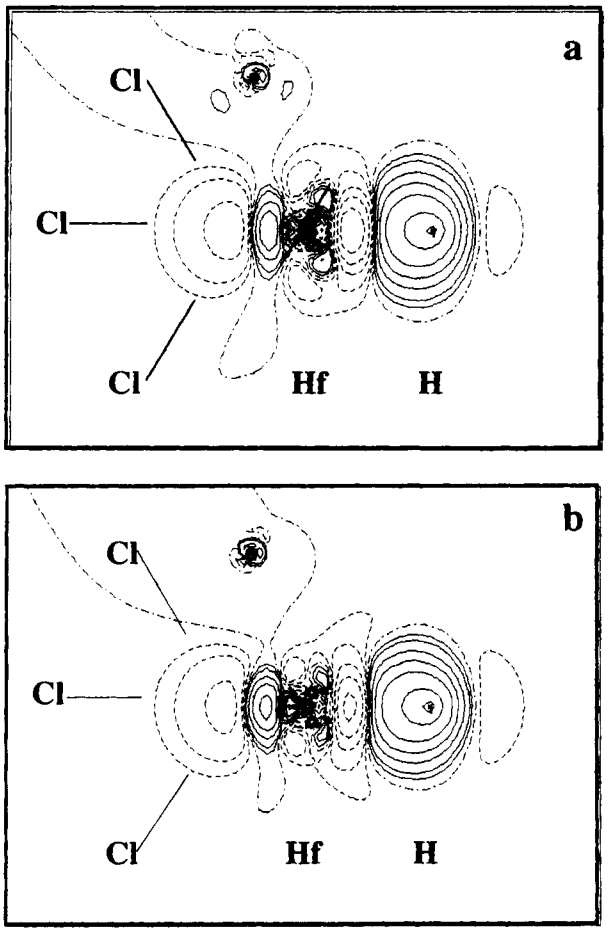

Figure 3. The deformation density $\Delta\varrho$ for $HfCl_3H$ from $HfCl_3$ and H: (a) $\Delta\varrho^{NR}$; (b) $\Delta\varrho^{QR}$. Densities are plotted in the *xz* plane: drawn lines, positive; dashed lines, negative; dash-dotted lines, zero. Contour values (atomic units)SPCLN 0.5, 0.2, 0.1, 0.05, 0.02, 0.01, 0.005, 0.002, 0.001, 0.0, −0.001, −0.002, −0.005, −0.01, −0.02, −0.05, −0.10, −0.20, −0.50.

$HfCl_3H$ indicates a loss of 0.23e in 6s on formation of the Hf−H bond whereas the corresponding loss in 5d only is 0.02e. This analysis indicates that the major part of the charge transfer from the metal to hydrogen comes from 6s, just as in the nonrelativistic case.

The nonrelativistic $6a_1$ bonding orbital, **4a**, underlines the polarization of the Hf−H bond with a 59% contribution from H 1s, Table 4. The major metal contribution (22%) to $6a_1$ comes from 5d. The $6a_1$ orbital is only slightly modified by relativity, **4b**. Now the polarization toward hydrogen has been reduced to a 53% contribution as the participating $6a_1^f$ FO orbital has been lowered in energy by relativity. We note that the $6a_1$ HOMO of $HfCl_3H$ is made up of the $6a_1^f$ FO and H 1s with hardly any contribution from the other fragment orbitals of $HfCl_3$, Table 4.

The effect of bonding to H can be illustrated by a plot of the deformation density $\Delta\varrho$, defined as $\Delta\varrho = \varrho_{Cl_3HfH} - \varrho_{Cl_3Hf} - \varrho_H$. The deformation densities $\Delta\varrho^{NR}$ and $\Delta\varrho^{QR}$ are given in Figure 3. They clearly show the decrease in 6s and increase in H 1s character, whereas the change in 5d character is hardly visible. The deformation densities are very similar: the NR and QR bonds to H are practically equal.

Table 5 provides an energy analysis of the Cl_3Hf−H bond by the ETS method[13a] according to the decomposition scheme outlined in eqs 1−3. We find that the QR scheme with $D_e(Cl_3Hf-H) = 3.77$ eV (86.9 kcal/mol) affords a stronger bond than the NR method with $D_e(Cl_3Hf-H) = 3.51$ eV (80.9 kcal/mol).

Table 5. Energy[a] Analysis for $HfCl_3H$ and $ThCl_3H$

	$HfCl_3H$ from $HfCl_3$ and H				$ThCl_3H$ from $ThCl_3$ and H			
	NR[b]		QR[b]		NR[b]		QR[b]	
$\Delta E_{el.stat}$	−2.76		−2.79		−1.40		−1.74	
ΔE_{Pauli}	2.35		2.20		2.43		1.98	
ΔE^0		−0.42		−0.60		1.03		0.24
ΔE_{A_1}	−3.33		−3.43		−3.01		−3.84	
ΔE_{A_2}	0.0		0.0		0.00		0.00	
ΔE_{E_1}	0.01		0.01		0.03		0.02	
ΔE_{oi}		−3.09		−3.18		−3.00		−3.83
ΔE		−3.51		−3.77		−1.97		−3.60

[a] Energies in eV. [b] Based on geometries optimized by QR.

It follows from the analysis in Table 5 that relativity enhances the Hf−H bond energy by making the orbital interaction, ΔE_{oi}, more favorable (negative) and the Pauli repulsion, ΔE_{Pauli}, less destabilizing (positive), Table 5.

The orbital interaction energy ΔE_{oi} is more stabilizing in the QR case as a result of ΔE_{A_1} which is the dominating term in the decomposition of ΔE_{oi}, Table 4. The ΔE_{A_1} term is enhanced by relativity since the FO $6a_1^f$ and H 1s levels are closer in energy in this QR case, and thus better able to interact.

The relativistic reduction in the Pauli repulsion term, ΔE_{Pauli}, is a general phenomenon.[3] In the case at hand, the 1s electron penetrates to some degree the core region of Hf as H and $HfCl_3$ are brought together. The penetration results in high instantaneous velocities of the intruding electron around the Hf nucleus since the H 1s orbital must remain orthogonal to the Hf core orbitals as a result of the Pauli exclusion principle. The outcome is an increase in the kinetic energy and a sizable repulsive contribution to ΔE_{Pauli}. However, relativity will diminish this contribution by reducing the kinetic energy in much the same way as it reduced the kinetic energy of the $(n + 1)$s orbital and lowered its energy.[3] A more detailed description of how relativity reduces ΔE_{Pauli} can be found elsewhere.[3,19]

(e) The Cl_3Th−H Bond. From the population analysis of Table 6 we see that the interaction between $ThCl_3$ and H takes place predominantly in the $6a_1$ orbital, **5a** (NR) and **5b** (QR).

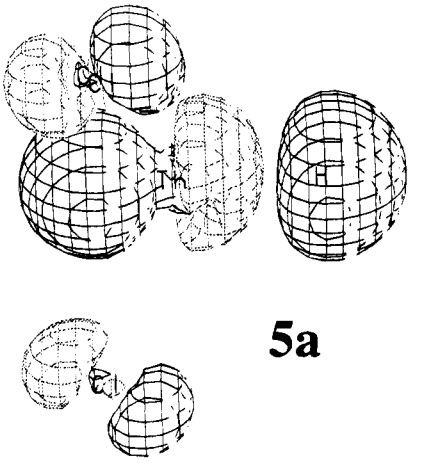

It is not possible to talk about a single $ThCl_3$ fragment orbital contributing to the bond in $6a_1$. The singly occupied $6a_1^f$ orbital, which was the major contributer to the Cl_3Hf−H bond, is supplemented in $ThCl_3H$ by additions from $7a_1^f$, $8a_1^f$, and $9a_1^f$. In fact, $6a_1^f$ does not contribute to $6a_1$ in the NR case since it is made up of the $5f_\phi$ orbital, Tables 3 and 6.

(19) Ziegler, T.; Snijders, J. G.; Baerends, E. J. *ACS Symp. Ser.* **1989**, *395*, 322.

Table 6. Population Analysis of Highest Occupied A_1 Orbitals of $ThCl_3H$

NR	Orbital	Orbital char.	Energy	%Th-contribution				%$ThCl_3$					%H
			(eV)	7s	d_σ	f_σ	f_ϕ	$4a_1^f$	$5a_1^f$	$7a_1^f$	$8a_1^f$	$9a_1^f$	
	$6a_1$	$5f_\sigma$,6d -H b.	-6.27	1	14	15			6	17	20	1	56
	$5a_1$	$5a_1^f$-H b.	-7.97	1	4	5	1		94	7			4
	$4a_1$	$4a_1^f$	-8.55	1	7		8	99					
Gross Populations				0.07	0.52	0.42							1.24

QR	Orbital	Orbital char.	Energy	%Th-contribution				%$ThCl_3$						%H
			(eV)	7s	d_σ	f_σ	f_ϕ	$4a_1^f$	$5a_1^f$	$6a_1^f$	$7a_1^f$	$8a_1^f$	$9a_1^f$	
	$6a_1$	6d,7s,$5f_\sigma$, -H b.	-6.43	5	18	2			5	19	13	1	2	61
	$5a_1$	$5a_1^f$-H b.	-8.12	1	8	2			95	1				3
	$4a_1$	$4a_1^f$	-8.98	6	3	1	3	99						1
Gross Populations				0.30	0.60	0.10								1.37

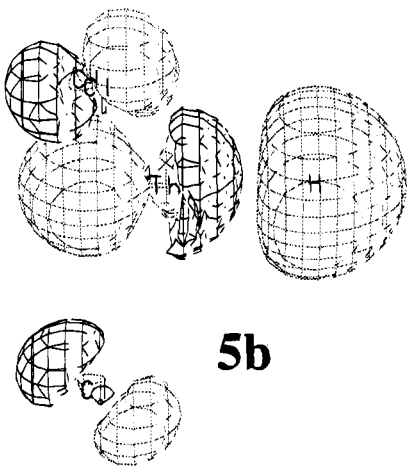

5b

Looking at total populations in $ThCl_3$ and $ThCl_3H$, we find in the NR case a decrease in f character from 0.99e in $ThCl_3$ to 0.42e in $ThCl_3H$. The s character is decreased too (0.09e vs 0.07e). The d population increases, on the other hand, considerably from 0.16e to 0.52e. The relative increase in 6d character at the expense of 5f can be explained by the fact that the Th 6d to H 1s interaction matrix element numerically is larger than the elements involving $5f_\sigma$, in line with the relative ordering **1g** > **1h** of the corresponding overlaps. Thus, $6d_\sigma$ is drawn into the bonding because of the good interaction with H 1s, although it is of higher energy than $5f_\sigma$, Figure 2. One might have expected a contribution from 7s in view of the large overlap with H 1s, **1f**. However, 7s is relatively high in energy, Figure 2, and its interaction with H 1s weaker than the $5d_\sigma$ interaction.

The nonrelativistic $6a_1$ bonding orbital, **5a**, underlines again the polarization of the Th−H bond with a 56% contribution from H 1s, Table 6. The major metal contributions comes from $6d_\sigma$ (14%) and $5f_\sigma$ (15%). The metal composition in $6a_1$ differs considerably from that of the $6a_1^f$ and $7a_1^f$ NR fragment orbitals in $ThCl_3$ with nearly 100% f character.

The relativistic $ThCl_3$ fragment has 0.79e in 7s, 0.41e in $6d_\sigma$, and only 0.27e in 5f, Table 3. This is in contrast to the NR $THCl_3$ fragment, where almost all of the metal charge is in 5f. The change reflects the relativistic destabilization of 5f compared to 6d and in particular 7s, Figure 2. One might have expected the 7s orbital also to dominate the bonding in the relativistic calculations on $ThCl_3H$. In fact, we find a loss in 7s character of 0.49e and a gain of 0.29e for 6d in going from $ThCl_3$ to $ThCl_3H$. The total 5f content, on the other hand, remained nearly equal. Again, the matrix element between $6d_\sigma$ and 1s H is numerically larger than the corresponding element involving 7s. Thus, $6d_\sigma$ is drawn into the bonding although it is of higher energy than 7s.

The relativistic $6a_1$ orbital accounting for the Th−H bond in Cl_3Th−H, **5b**, has a 61% H 1s contribution and is thus more polarized than its nonrelativistic counterpart with 56% H 1s contribution, Table 6. The loss in metal contribution is a result of the relativistic 5f destabilization. Thus the 5f contribution is reduced from 15% to 2% in going from NR to QR. By contrast, the 7s population is increased from 1% to 5% and the 6d participation from 14% to 18%.

Density difference plots for $\Delta\varrho^{NR}$ and $\Delta\varrho^{QR}$ are given in Figure 4. Surprisingly they look very similar, although the number and appearance of the contours are different. The following effects from the bonding to H can be seen: the increase in H 1s population and in the NR case a substantial loss of f_σ character and a (smaller) increase in d_σ character, visible from the depletion along the Th−H axis. In the QR case the loss of 7s character can be seen, as well as the other effects, decrease in f_σ character and increase in d_σ character. The NR $ThCl_3$ density was based on a population of $7a_1$ ($5f_\sigma$) instead of $6a_1$($5f_\phi$).

The relativistic Cl_3Th−H bond energy of 3.60 eV (82.8 kcal/mol) is nearly twice as large as the nonrelativistic bond energy of 45.4 kcal/mol. An experimental estimate of the Th−H bond in Cp_2ClTh−H by Bruno[20] et al. affords a value of 80 kcal/mol. The terms ΔE_{Pauli}, $\Delta E_{el.stat}$, and ΔE_{oi} all contributes to the difference between NR and QR. An analysis of the trends

(20) Bruno, J. W.; Stecher, H. A.; Mors, L. R.; Sonnenberg, D. C.; Marks, T. J. *J. Am. Chem. Soc.* **1986**, *108*, 7275.

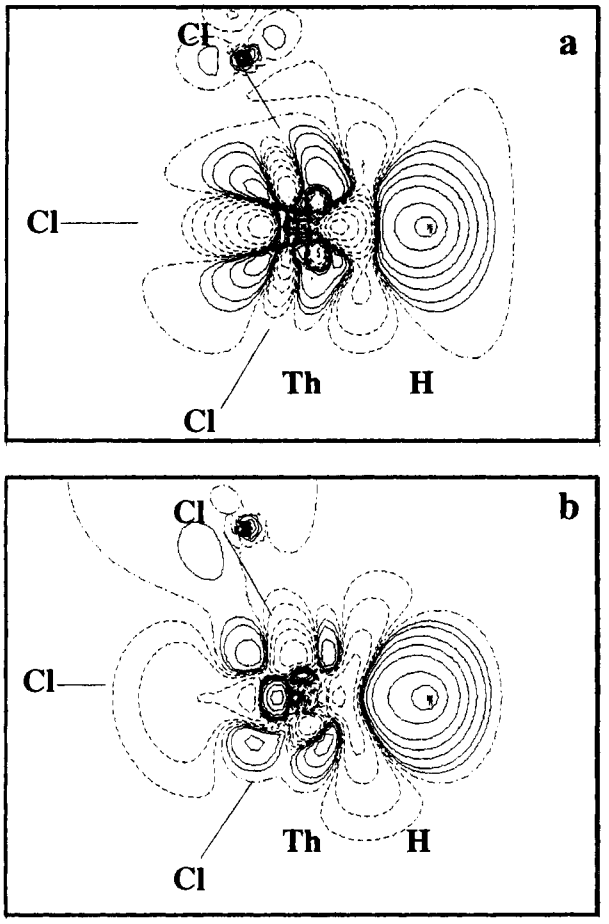

Figure 4. Deformation density $\Delta\varrho$ for $ThCl_3H$ from $ThCl_3$ and H: (a) $\Delta\varrho^{NP}$; (b) $\Delta\varrho^{QR}$. Densities are plotted in xz plane: drawn lines, positive; dashed lines, negative; dash-dotted lines, zero. Contour values (atomic units)SPCLN 0.5, 0.2, 0.1, 0.05, 0.02, 0.01, 0.005, 0.002, 0.001, 0.0, −0.001, −0.002, −0.005, −0.01, −0.02, −005, −0.10, −0.20, −0.50.

is complicated by the fact that the NR and QR frontier orbitals differ considerably.

The relativistic reduction in ΔE_{Pauli} can in part be accounted for by the corresponding reduction in the kinetic energy, an effect discussed previously in connection with $HfCl_3H$. The more stabilizing (negative) relativistic $\Delta E_{el.stat}$ term is related to the fact that $6a_1^f$ in the QR case is 7s based whereas the $ThCl_3$ frontier orbitals in the NR case are of 5f character. The 7s orbital does not shield the Th nucleus as well as 5f, thus allowing for a more attractive electrostatic interaction between H and the $ThCl_3$ fragment.

The orbital interaction term, ΔE_{oi}, is again dominated by ΔE_{A_1} and it makes the Th−H bond stronger by 19 kcal/mol in the QR case. The distinction in the strength of the two bonds can be related to the different way in which charge is redistributed on the metal center in the NR and QR cases. The nonrelativistic Th−H bond formation involves a redistribution of charge (0.36e) on the metal center from 5f to 6d in order to enhance the interaction with H 1s. This is costly since 5f is placed below 6d by 5 eV, Figure 2. The relativistic Th−H bond formation involves, on the other hand, polarization of charge (0.29e) from 7s to 6d. The 7s to 6d transfer cost less in energy due to the closer proximity (1.32 eV) of the two orbitals. Thus, the difference in Th−H bond strength is ultimately related to the relativistic stabilization of 7s and destabilization of 5f.

Conclusion

We have studied the covalent Ac−X σ-bond modeled by Cl_3-Th−H and compared it to the related Cl_3Hf−H bond involving the early 5d transition metal hafnium.

Our investigation has shown that the bonding between the transition metal fragment $HfCl_3$ and H largely involves the 5d orbital with a modest contribution from 6s. Relativity tends to stabilize 6s, and thus this orbital is more important in QR than in NR. The preference for 5d over 6s stems from the numerically larger interaction matrix element between the former orbital and H 1s. The relativistic contribution to the Cl_3Hf−H bond is 6 kcal/mol.

On the other hand, the bonding between the actinide fragment $ThCl_3$ and H exhibits very different characteristics in the NR and QR schemes. In the NR calculation, we have a bond with equal participations from 6d and 5f, whereas 6d is the only important participating metal orbital at the QR level with only smaller contributions from 5f and 7s. Relativity increases the Th−H bond strength by 42 kcal/mol. It can be argued that the Hf−H and Th−H bonds are quite similar after relativistic effects have been included in the description.

Acknowledgment. This investigation was supported by the Natural Sciences and Engineering Research Council of Canada (NSERC) as well as the donors of the Petroleum Research Fund, administered by the American Chemical Society (Grant ACS-PRF 27023-AC3).

IC940343W